

4D Printing on Textiles: Developing a File to Fabrication Framework for Self-Forming, Composite Wearables



Asterios Agkathidis and Guzden Varinlioglu

This design-led research investigates the development of self-forming wearable composite structures by 3D printing semi-elastic embossed patterns out of semi-elastic Thermoplastic Polyurethane 95 (TPU95) filament on pre-stretched textiles and releasing the stress after the printing has been completed. In particular, the study present and compare two methods of ‘file to fabrication’ techniques for generating self-forming textile shell structures: The first is based on printed patterns related to their stress line simulation and the second on modified geometrical patterns in relation to their curvature analysis. Furthermore, we will investigate the buckling degree of the composites in relation to their fabric thickness and elasticity. The findings emphasise the advantages and challenges of each method as well as presenting a comparative table chart highlighting the relationship between material properties, pattern geometry and the formal vocabulary of the composite shells.

1 Introduction

At the beginning of the twentieth century, debates and developments which significantly changed the character of geometry gained momentum. By 1921, Albert Einstein questioned the relationship between geometry and experience, logical-formal language and real-life experience, and added physics as a complementary

A. Agkathidis (✉)

Liverpool School of Architecture, University of Liverpool, 25
Abercromby Square, Liverpool L69 7ZN, UK
e-mail: asterios.agkathidis@liverpool.ac.uk

G. Varinlioglu

Department of Architecture, Izmir University of Economics,
Sakarya Street, 156 35300 Balçova, Izmir, Turkey

thinking tool to understand the universe, which he called practical geometry [1]. The notion of geometry, which is meant to measure the Earth and initially connect it with realworld experience, turned away from reality into a logical and formal thought system, and in the early twentieth century, the relationship between geometry and experience became more questionable. Against the tendency to reduce geometry to logical and formal axioms, Buckminster Fuller proposed to reconsider orthogonal and cartesian geometry in relation to action, operation and movement [2]. He questioned geometry with different conceptions introducing the notion of folding as ‘a way of thinking’, ‘folding as a form of action and operation’ and ‘folding by action’. Beyond the concept of geometry being reduced to static and rigid axioms, Buckminster Fuller placed movement at the centre, conceptualising it as self-provoking and self-initiating.

Frei Otto continued this approach with his research on doubly curved fabric structures during the 1970s and 1990s. Otto’s design and form-finding process were strongly relying on physical models, rather than computational methods. Having developed a large range of innovative structures, by the early 1990s, Otto et al. [3] declared:

Our times demand lighter, more energy-saving, more mobile and more adaptable, in short, more natural buildings, without disregarding the demand for safety and security.

In the early 2000s, others such as Brown and Rice [4] at Arup, focused on computational methods and techniques which they were applying for material innovation stress analysis and form-finding. Those developments continued in the 2010s with membranes and textiles being used successfully in building construction in the form of roofs, facades, pneumatic structures and tents. In our times, the rapid development of emerging technologies such as 3D printing and additive manufacturing, plus developments in material science, are enabling designers to consider further innovative solution synergies expanding its applicability to a wide facette of complexity and materiality such as plastics, concrete and metals. While 3D printing has been experiencing rapid development in the past two decades, the notion of four-dimensional printing has only appeared in 2012 according to Wu et al. [5]. The term describes the process through which a 3D printed object transforms its shape and structure over the influence of environmental parameters (e.g. temperature, humidity, light) or material properties (e.g. digital shape memory or stress relaxation), whereby the fourth dimension of the printing process becomes time.

In continuation of the previous work by the authors on ‘3D printing of elastic fibre patterns on pre-stretched textiles’ [6] and ‘architectural hybrid material composites, computationally enabled techniques to control form generation’ [7], this paper investigates the possibilities arising in shape, material properties and geometry of objects produced, by 3D printing of semi-elastic Thermoplastic Polyurethane 95 (TPU 95) onto pre-stretched elastic fabric (e.g. lycra-spandex) as shown in Fig. 1.

In particular, two different form prediction/form-finding methods were applied as described by Agkathidis et al. [6] and Berdos et al. [7] and tested in their effectiveness in predicting the desired shape and their suitability and limitations for producing particular geometries. Furthermore, the two methods were assessed and verified by

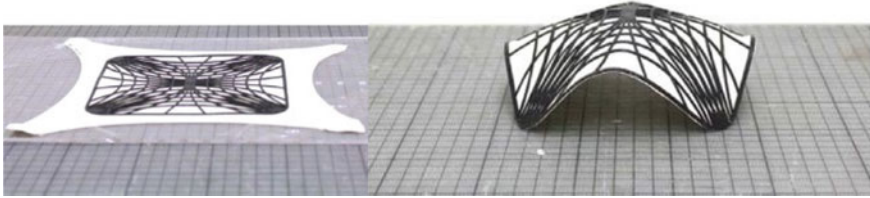


Fig. 1 This image illustrates the flat 2D pattern and resulting 3D geometry after release

using three different 3D printers (an Ultimaker-3 and the low-cost JG Aurora A5, Zaxe) allowing both to print directly on different fabrics, such as Polyamide Nylon and Elastane, Modal and Elastane composites, easily consumable wearables in the textile industry. Consequently, the following research questions were investigated:

- Which of the two proposed methods assessed here are more effective in controlling and predicting the form and performance of hybrid panels composed of semi-flexible, pattern fibres printed onto flat elastic, pre-stretched textiles?
- How do the material properties of the individual components—the textiles and the fibres—contribute to the properties of the composite material?
- How does the elasticity and thickness of the textile and the filament affect the degree of buckling of the final geometry?

To answer the above questions, a set of design-led, physical experiments were conducted using the two different form prediction methods on the three different printers and on different textile materials by developing a set of composite wearable prototypes. The findings were analysed and compared to enable conclusions.

2 Background and Literature

The study began by looking into the related work of other researchers in order to inform our research of the latest developments in the field. In their research, Joshi et al. [8] presented various active materials, 4D printing techniques and shape memories, however, their approach was mostly emphasising the field of structural engineering as they were focusing less on design. Cheng et al. [9, 10], describe the development of an additive manufacturing method combined with fused granular fabrication capable of producing 4D printed meta-structures, out of biocomposite material, which can change their geometry from flat to curved in relation to the environmental humidity. However, their work is using a completely different material pallet, to the ones examined in this paper.

Meyer et al. [11] investigated the adhesion of 3D printed polylactic acid (also known as PLA) on textile fabrics while Redondo et al. [12] researched the adhesion of 3D printed PLA samples on fabric by using the Fused Deposition Modeling

technique. Even though both works provide valuable insights into the material properties and behaviour of PLA printed on fabric, they are neither examining the formal behaviour of the 3D printed objects nor their capability to change in time.

'Additive Manufacturing and Textiles' by Sitotaw et al. [13] broad overview casts light on various 3D printing techniques related to textiles, however, it was mostly focused on understanding material and technique properties rather than introducing novel materials and methods. Ehrmann and Ehrmann [14], presented their research on the 'Shape-Memory Properties of 3D Printed PLA Structures' which similarly to Giglio et al. [15] focuses on 3D printed PLA fabrics rather than on composites of PLA structures printed on textiles.

The prototypes produced in the workshop by Erioli and Naldoni [16] explored the possibilities in form generation by 3D printing semi-elastic PLA patterns on pre-stretched textiles. However, their investigation remained at an empirical level, which appears to emphasise artistic over empirical qualities, without incorporating simulation methods and form-prediction mechanisms. A similar technique was previously presented by Guberan and Clopath [17], in their 'Active Shoes' project, where a 3D printed geometry on a pre-stretched textile surface allowed the creation of a controlled and predictable shoe. However, there it might have not been their intention to provide evidence of simulation or form-prediction tools being used either.

In their article 'Printing on Fabric Meta-Material for Self-Shaping Architectural Models', Jourdan et al. [18] described a novel method of 3D printing PLA bars on pre-stretched textiles, including a star-based pattern system as well as a novel technique to simulate and predict the final shape of the models. However, they were not revealing the software and the tools used which are certainly different to the ones applied in this research. Their work offers a useful opportunity to compare the different methods in relation to their effectiveness.

In addition, Koch et al. [19], gave an overview of recent techniques for the generation of 4D textiles made by additive manufacturing on pre-stressed textiles offering a valid database for categorising, evaluating and assessing the techniques and methods of our research.

In their 'FabriClick' article Goudswaard et al. [20] showed a method for interweaving push buttons into fabrics by using 3D printing and digital embroidery. Even though they were achieving similar effects as described in our research, they don't seem to be using form prediction techniques such as stress line simulation and curvature analysis in their design process. A similar approach is described by Kycia [21], in the research on 3D printing on pre-stressed fabrics in order to create textile composites and explore their potential applications as building envelopes. Kycia has explored PLA, as well as polyolefin filaments on smaller as well as scale prototypes. Kycia showed rather simple, hyperbolic paraboloid geometries, without presenting any computational, form predicting methods. Finally, the research described by Aldinger et al. [22] in the 'Tailoring Self-Formation' paper has common ground with our work. However, finite element analysis appears to be their main tool of form prediction. In their material studies, carbon fibre rods were knitted into the fabric and helped to better control the self-formation geometry but they are not 3D printing filament on the textiles in order to produce the composite shapes.

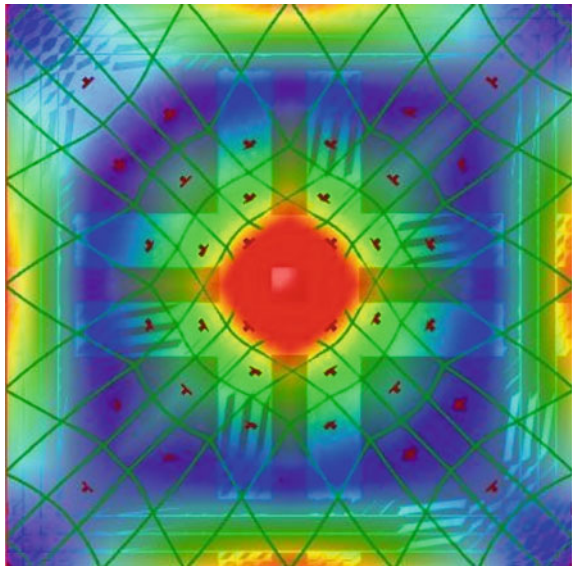
The conclusion deriving from the literature review on similar research is that 4D printing on textiles is an up and coming research field that is currently being investigated by many research groups around the world. However, even though researchers have applied various methods and techniques of 4D printing and form prediction, our research appears to offer an original approach to the field as it is applying materials and methods not described by any of the researchers.

3 Development of Materials and Methods

As previously described, two different form-prediction methods were applied and tested for developing pattern geometries which we were then 3D printed on pre-stressed textiles. By releasing the newly composed prototypes, the objects should self-form into the desired wearable shape. Both methods have been developed using parametric tools (*Rhinoceros and Grasshopper*). In particular, Method 1 is based on utilising the Mean curvature analysis of the digital design model and adjusting geometric patterns on it by using an algorithm incorporating the Panelling Tools plug-in for Grasshopper (Fig. 1). The modified pattern is then being flattened, embossed and printed onto the pre-stressed textile.

Method 2 is based on an algorithm incorporating the *Karamba* structural simulation plug-in for *Grasshopper* [6], capable of conducting stress line simulations on the desired, digital design model (Fig. 2). The stress lines were rationalised and converted into a pattern which was then flattened, embossed and printed onto the pre-stressed textile.

Fig. 2 Diamond pattern adjusted according to Mean curvature map of a curved surface (Method 1)



Both methods were tested by conducting four experiments, where three types of wearable objects, bracelet/coffee cup holders, hats and facemasks/extensions were designed and fabricated. The first set of experiments (1, 2, 3, 4) measured the displacement between digital and physical models, thus the effectiveness of each method was verified, as well as identified the parameters which may influence the form prediction/generation. The study utilised an Ultimaker-3 3D printer, semi-elastic Thermoplastic Polyurethane 95 (TPU 95) filament and a Lycra Spandex 240 gms textile with a 40–20% stretch in the X and Y directions. In addition, the second set of experiments (5, 6, 7, 8) will examine the buckling capacity of the composite objects in relation to the use of different textile types such as Polyamide Nylon and Modal with different percentages of Elastane and thicknesses as well as to the embossed filament pattern (TPU95) by applying Method 2. The study tested the effectiveness of two low budget printers Zaxe and JG Aurora A5 printers, semielastic, which will be utilised for the second set of experiments, as well as the assembly method on the textile (either directly printed on the fabric or being laminated to it afterwards).

4 Verification Through Design Experiments

4.1 Experiment 1

Experiment 1 examined the design of a cylindrical bracelet/coffee cup holder with a single curvature geometry which was developed using Method 1. A hexagonal and a diamond-shaped pattern is applied to the bracelet model and adjusted to its Mean curvature analysis map as illustrated in Fig. 3. The pattern density was increased in the flattest areas (blue) and decreased in the areas with the highest curvature (red).

This experiment consisted of six variants, where pattern parameters such as rod thickness, pattern shape as well as the existence (or not) of a boundary rod were being tested and compared to the original, digital 3D model (Fig. 4). Variant v1.1 was designed using a hexagonal pattern with a rod thickness of 2.5 mm without a boundary frame and did not bend to the desired shape. Variant v1.2 has a rod thickness of 2 mm and a diamond-shaped pattern while variant v1.3 used exactly the same pattern as v1.2 but its rod thickness is 2 mm. While v1.3 over-performed by curving more than expected, v1.2 did not curve enough. Variants v1.4, v1.5 and v1.6 were all alterations of the diamond pattern with a boundary, differing only in their rod thickness (2, 2.5, 1.8 mm) with v1.6 proving to be the closest to the preferred shape. The conclusion deriving from experiment 1 was that Method 1 allowed the successful reproduction of the desired shape with variant v1.6 showing the smallest discrepancy to the digital 3D model (Fig. 5).

Fig. 3 Stress line simulation pattern produced on a curved surface (Method 2)

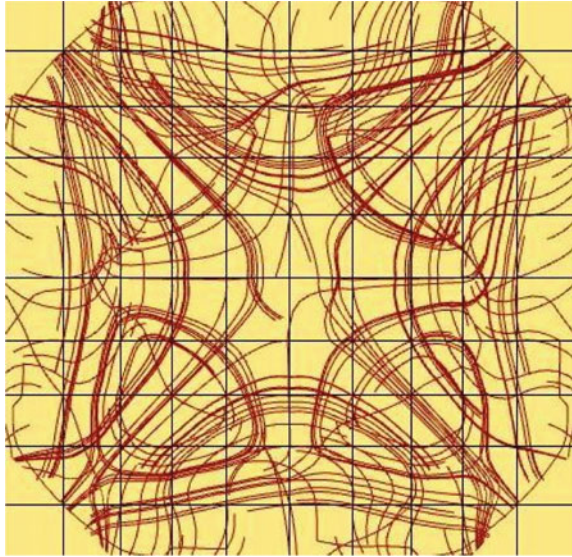


Fig. 4 Experiment 2, pattern adjustment on Mean curvature map (Method 1)

4.2 *Experiment 2*

Experiment 2 examined the design of a cylindrical bracelet/coffee cup holder with a single curvature geometry which was developed using Method 2. By applying the stress line simulation on the digital model, the stress line simulation pattern is generated as described in Fig. 6.

After being flattened, the stress lines were rationalised and transformed into a pattern that was embossed and 3D printed on the pre-stressed fabric. Two variants were tested. Variant v2.1 had a lower density stress line pattern with a rod thickness of 1.5 mm. Variant v2.2 had a higher density stress line pattern with a rod thickness of 1.5 mm. Both variations have an outer frame with a 1.5 mm thickness (Fig. 7). The conclusion deriving from experiment 2 was that Method 2 allowed the successful reproduction of the desired shape with variant v2.2 showing the smallest discrepancy to the digital 3D model (Fig. 7).

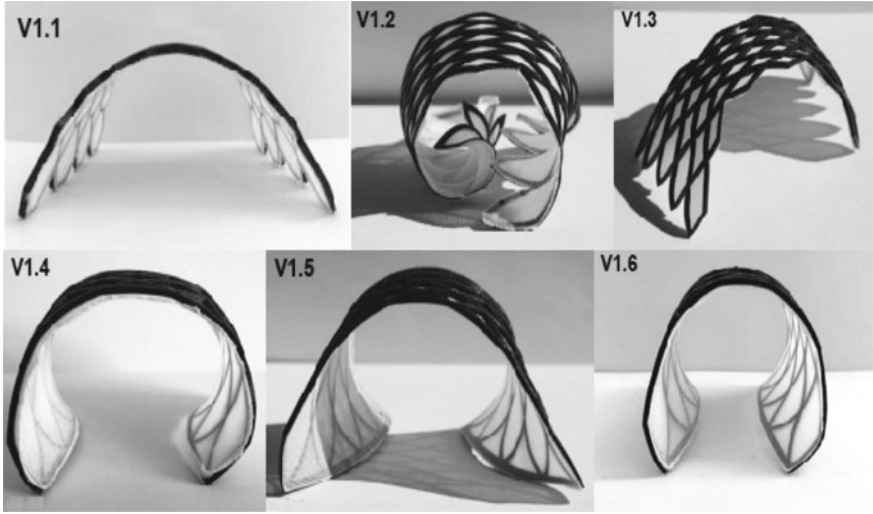


Fig. 5 Experiment 1, and the variants v1.1, v1.2, v1.3, v1.4, v1.5 and v1.6

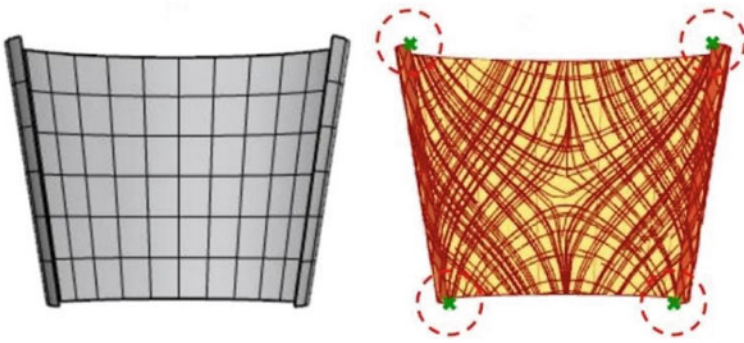


Fig. 6 Experiment 2, pattern generation via stress line simulation (Method 2)

4.3 Experiment 3

Experiment 3 examined the design of a facemask with a double curvature geometry which was developed using Method 1. We produced four variants as displayed in Fig. 8. Variant v3.1 is formed of a 3:3 diamond-shaped pattern with a rod thickness of 2 mm, variant v3.2 of a 4:4 diamond-shaped pattern with a rod thickness of 1 mm, variants v3.3 and v3.4 of a 5:5 and 6:6 diamond-shaped pattern accordingly, both having with a rod thickness of 1 mm. None of the variants has adopted a boundary frame.



Fig. 7 Experiment 2, variants v2.1 and v2.2

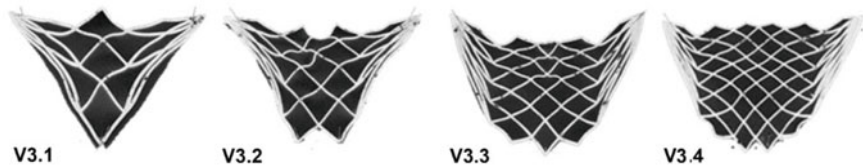


Fig. 8 Experiment 3, variants v3.1, v3.2, v3.3, v3.4

The conclusion deriving from experiment 3 was that Method 1 did not allow the successful reproduction of the desired shape, in particular in the z-direction, where the objects did not curve as expected.

4.4 Experiment 4

Experiment 4 examined the design of a facemask with a double curvature geometry which was developed using Method 2. Four variants were produced, as displayed in Fig. 9. Variant v4.1 applied a 40% stretch and has a rod thickness of 1 mm, variant v4.2 a 35% stretch with a rod thickness of 1.5 mm, variants v4.3 and v4.4 of a 30 and 25% stretch accordingly, both having a rod thickness of 2 mm. While variants v4.1, v4.3 and v4.4 have adopted a boundary frame, variant v4.2 has no boundary frame.

The conclusion deriving from experiment 4 was that Method 2 did allow the successful reproduction of the desired shape with variant v4.4 (including the boundary) showing the smallest discrepancy from the desired shape. Furthermore, variant v4.2 without a boundary border was the least successful variant in comparison to all other three variants which included a boundary border.

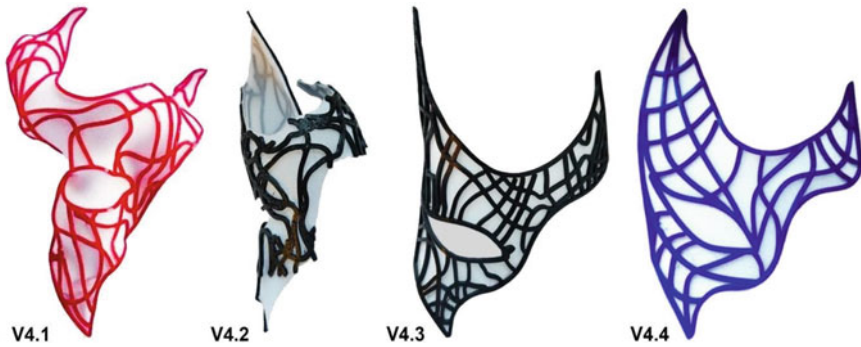


Fig. 9 Experiment 4, variants v4.1, v4.2, v4.3, v4.4



Fig. 10 Experiment 5, variants v5.1, v5.2, v5.3

4.5 Experiment 5

Experiment 5 examined the design of a cylindrical bracelet/coffee cup holder with a single curvature geometry using Method 2 and was printed on two different textiles with different stretching percentages. Variant v5.1 applied a 40% stretch of a silky matt transparent textile of 15 denier thickness (83% Polyamide, 17% Elastane), while v5.2 applied a 30% stretch of the matt opaque textile of 40 denier thickness (86% Polyamide, 14% Elastane) while v5.3 applied a 20% stretch of the same textile. All patterns have the same rod height (2 mm) but different rod thicknesses, v5.1 has a rod thickness of 1 mm, variant v5.2 with a rod thickness of 2 mm, variant v5.3 with a rod thickness of 3 mm (Fig. 10). The 3D prints of all variants v5.1, v5.2 and v5.3 were printed using a JC 3D printer directly on pre-stretched textiles. The conclusion deriving from experiment 5 was that all three textiles delivered a decent degree of buckling, which is strongly related to the rod thickness and density of the composite structure.



Fig. 11 Experiment 6, variants v6.1, v6.2, v6.3

4.6 Experiment 6

Experiment 6 examined the design of a face mask with a double curvature of a complete geometry (with boundaries) which was developed using Method 2 and will be printed on two different textiles using a variety of pattern geometries. All three variants (Fig. 11) were produced by the same printing method and the stretching factor applied was the same. Three similar textiles with a slight difference in thickness and the same rod thickness/height (1 mm of rod thickness and height) were used. Variant v6.1 utilised a sheer and shiny 80% Polyamide and 20% Elastane fabric with a thickness of 5 deniers. Variants v6.2 and v6.3 utilised an opaque mat of slightly thicker, 83% Polyamide, 17% Elastane textile with a thickness of 40 deniers. All three variants described closed, curvilinear shapes (circle, free form, and ellipse) with different 3D printed patterns. The distribution and density of the stress lines—equal in x and y dimensions—varied. The conclusion deriving from experiment 6 was that the thinner textiles delivered a higher degree of buckling, in comparison to the previous experiment (experiment 5).

4.7 Experiment 7

Experiment 7 examined a doubly curved face mask (with boundary borders) which was developed using Method 2 and was printed on two textiles with different thicknesses using different assembly methods. One of the two textiles used was 20 deniers thick composed out of 82% Polyamide and 18% Elastane, while the second one was 40 deniers thick composed out of 6% Polyamide and 14% Elastane. The embossed patterns had different thicknesses as well, but with the same rod height (Fig. 12). The textile of both v7.1 and v7.3 variants had a thickness of 20 deniers. Both v7.2 and v7.4 were applied on an opaque mat and slightly thicker textile (40 deniers). In both v7.1 and v7.2 variants, the patterns were printed directly on the fabric. Variants v7.2 and v7.4 were laminated on the fabric by using mitral Cyanoacrylate Adhesive glue. The distribution and density of the stress lines varied, as well as their rod thickness and height. The conclusion deriving from experiment 7 was that the objects where



Fig. 12 Experiment 7, variants v7.1, v7.2, v7.3, v7.4 (v7.1 and v7.2 used the same assembly method, while v7.1 and 7.3 used the same textile)



Fig. 13 Experiment 8, variants v8.1, v8.2, v8.3

the filament was printed directly on the textile have performed better (higher buckling degree) than those who were laminated on the fabrics after the printing had been completed (lower buckling degree).

4.8 Experiment 8

Experiment 8 examined a double curvature face mask that was developed using Method 2 and was printed on three different textiles with similar stretching percentages. Variant v8.1 was applied on a matt opaque tights fabric of 40 deniers thickness (92% Polyamide, 8% Elastane), while v8.2 was applied on a textile of 80 deniers thickness (91% Polyamide, 9% Elastane) and v8.3 on a modal textile (92% modal, 8% Elastane), all utilising patterns with the same rod height and thickness (Fig. 13). The 3D prints of all variants 8.1, v8.2 and v8.3 were printed using a Zaxe printer bed and the printed patterns were laminated on the pre-stretched fabric. Our conclusion from experiment 8 is that the thinner textiles delivered a higher degree of buckling.

5 Findings

The findings regarding the performance of the different methods are presented in Tables 1 and 2, a comparative displacement chart between variants and the digital 3D models used to design them. It became evident that variants v1.6, v2.2, v3.4 and

Table 1 Variation size displacement chart in mm

Variations	Stretch (%)	Material thickness (mm)	X dimension (mm)	Y dimension (mm)	Z dimension (mm)	X/Y/Z displacement (mm)
V1 DM	–	NA	30	85	40	–
V1.1	40	2.5	102	80	57	+72/–05/+17
V1.2	40	2.0	51	79	59	+21/–06/+19
V1.3	40	2.5	95	75	60	+65/–10/+20
V1.4	40	2.0	35	75	50	+05/–10/+10
V1.5	40	2.5	37	76	56	+07/–11/+16
V1.6	40	1.8	33	74	44	+03/–09/+04
V2 DM	–	NA	58	61	57	–
V2.1	40	1.5	124	61	60	+66/00/+03
V2.2	40	1.5	55	61	58	–03/00/+01
V3 DM	–	NA	170	95	106	–
V3.1	40	2.0	152	94	15	–18/–01/–91
V3.2	40	1.0	152	85	20	–18/–11/–86
V3.3	40	1.0	152	94	5	–18/–01/–101
V3.4	40	1.0	152	95	10	–18/00/–96
V4 DM	–	NA	134	150	43	–
V4.1	40	1.0	82	120	38	–52/–30/–5
V4.2	35	1.5	61	139	41	–73/–11/–2
V4.3	30	1.5	101	148	43	–33/–02/0
V4.4	25	2.0	124	148	43	–10/–02/–0

v4.4 were the most successful cases of each experiment. Both of the tested methods proved to be performing to an acceptable level.

Despite no prototype having the exact measurements to the digital model it has derived from, it appeared that Method 2, linked to the stress line simulation delivered the smallest discrepancies in the double curvature experiment (experiment 4), with variant v4.4 differing only -7% in the X direction and -1% in the Y direction while showing no difference in the Z direction (Table 2). The findings were very similar in the single curvature experiment (experiment 2), with variant v2.2 differing only -3% in the X and $+2\%$ in the Z directions while showing no difference in the Y direction (Table 2).

The findings regarding the second set of experiments (5, 6, 7, 8) and the buckling performance of different textile type related composites are demonstrated in Table 3. It became evident that thinner textiles with a high percentage of elastane provided a higher degree of buckling (e.g. variants v5.1 and v7.1 with a thickness of 15 and 20 deniers accordingly). Furthermore, it appeared that rod height and thickness have a significant impact on the buckling degree. Overall, we have observed that the right

Table 2 Variation size displacement chart in %

Variations	X/Y/Z displacement in %
V1.1	+240/-6/+40
V1.2	+66/-6/+47
V1.3	+216/-12/+50
V1.4	+16/-12/+25
V1.5	+23 -13/+40
V1.6	+10/-09/+10
V2.1	+113/0/+5
V2.2	-3/0/+2
V3.1	-10/-1/-85
V3.2	-10/-11/-100
V3.3	-10/-1/-95
V3.4	-10/0/-90
V4.1	-38/-20/-12
V4.2	-54/-7/-5
V4.3	-24/-1/0
V4.4	-7/-1/0

combination of textile thickness and composition, as well as the distribution of stress line pattern and rod dimensions, play an essential role in reproducing the desired form and have to be chosen accordingly (e.g. v6.2). Finally, in our experiments, it became evident that printing on pre-stretched textiles directly helps the variants to deliver a higher degree of buckling as laminated variants, such as v8.1 and v8.2 deliver a smaller degree of buckling.

6 Conclusions

Our conclusions will focus on answering our research questions. Which of the two proposed methods assessed here are more effective in controlling and predicting the form and performance of hybrid panels composed of semi-flexible, pattern fibres printed onto flat elastic, pre-stretched textiles? Even though both methods appear effective to a certain degree, Method 2 based on patterns generated by stress line simulation is more efficient, in particular, when the object is double curved. This becomes evident in Tables 1 and 2, where the most accurately reproduced objects are variants v2.2 and v4.4, both doubly curved. Method 1, based on the curvature analysis and penalisation, proved successful in reproducing single curved objects, e.g. variant v1.6. However, it failed to deliver enough buckling in the z-direction in experiment 2.

Table 3 Textile buckling degree chart

	Initial form	Curvature	Dimensions <i>x/y</i>	Buckling in the <i>z</i> -direction	Printer	Rod thickness/height	Textile thickness	Textile description	Fabric type	Method of assembly
v5.1	trimmed rectangle with curved borders	single curvature	20 cm × 8 cm	7 cm	JG	1 m × 2 mm	15 deniers	Silky matt opaque tights, flat seams and 3D technology for a perfect fit	83% Polyamide 17% Elastane	Printed on textile
v5.2	trimmed rectangle with curved borders	single curvature	20 cm × 8 cm	8 cm	JG	2 mm × 2 mm	40 deniers	Silky matt opaque tights, flat seams and 3D technology for a perfect fit	86% Polyamide 14% Elastane	Printed on textile
v5.3	trimmed rectangle with curved borders	single curvature	10 cm × 23 cm	10 cm	JG	3 mm × 2 mm	40 deniers	Silky matt opaque tights, flat seams and 3D technology for a perfect fit	86% Polyamide 14% Elastane	Printed on textile
v6.1	Full circle	double curvature	15 cm diameter	3.5 cm	JG	1 mm × 1 mm	5 deniers	Ultra-sheer and shiny look flat seams tights	80% Polyamide 20% Elastane	Printed on textile

(continued)

Table 3 (continued)

	Initial form	Curvature	Dimensions x/y	Buckling in the z -direction	Printer	Rod thickness/height	Textile thickness	Textile description	Fabric type	Method of assembly
v6.2	free form	double curvature	25 cm × 15 cm	2 cm	JG	1 mm × 1 mm	15 deniers	Silky matt opaque tights, flat seams and 3D technology for a perfect fit	83% Polyamide 17% Elastane	Printed on textile
v6.3	deformed ellipse with full borders	double curvature	16 cm diameter	5.5 cm	JG	1 mm × 1 mm	15 deniers	Silky matt opaque tights, flat seams and 3D technology for a perfect fit	83% Polyamide 17% Elastane	Printed on textile
v7.1	Free form	double curvature	14 cm × 14 cm	10 cm	JG	2 mm × 1 mm	20 deniers	Sheer silky matt tights, flat seams	82% Polyamide 18% Elastane	Printed on textile
v7.2	Full circle	double curvature	15 cm × 15 cm	3.5 cm	JG	1.5 mm × 1.4 mm	40 deniers	Silky matt opaque tights, flat seams and 3D technology for a perfect fit	86% Polyamide 14% Elastane	Printed on textile
v7.3	Hexagon	double curvature	17 cm × 17 cm	11 cm	Zaxe	1.5 mm × 1.5 mm	20 deniers	Sheer silky matt tights, flat seams	82% Polyamide 18% Elastane	Laminated on textile
v7.4	Heart shape	double curvature	16.5 cm × 7.5 cm	8 cm	Zaxe	1.5 mm × 1.5 mm	40 deniers	Silky matt opaque tights, flat seams and 3D technology for a perfect fit	86% Polyamide 14% Elastane	Laminated on textile

(continued)

Table 3 (continued)

	Initial form	Curvature	Dimensions <i>x/y</i>	Buckling in the <i>z</i> -direction	Printer	Rod thickness/height	Textile thickness	Textile description	Fabric type	Method of assembly
v8.1	Ellipse	double curvature	17 cm diameter	2.8 cm	Zaxe	2 mm × 2 mm	40 deniers	Matt opaque tights	92% Polyamide 8% Elastane	Laminated on textile
v8.2	Full circle	double curvature	17 cm diameter	6.5 cm	Zaxe	2 mm × 2 mm	80deniers	matt opaque tights with 3D technology, water-resistant	91% Polyamide 9% Elastane	Laminated on textile
v8.3	Ellipse	double curvature	17 cm × 9 cm	3.3 cm	Zaxe	1 mm × 1 mm	Modal yarn	Transferring humidity very well	92% Modal 8% Elastane	Laminated on textile

How do the material properties of the individual components (the textiles and the fibres) contribute to the properties of the composite material? and how does the fibre pattern geometry influence the form of the composite hybrid panel? It appears that the relationship between textile type, rod thickness, stretching degree, pattern density and assembly method is very complex and particular, but also essential for reproducing the desired objects (Tables 1, 2, and 3). We could identify the following relationships: less dense patterns, operate best when directly printed on the textiles, on thinner and more elastic fabrics, while a bigger rod thickness and width is required in order to reproduce the object effectively.

How does the elasticity and thickness of the textile and the filament affect the degree of buckling of the final geometry? It appears that denser patterns, require thinner rod thickness and can deliver successful objects when printed on thinner, more elastic textiles. Overall, the elasticity and thickness of the textile are essential for both methods applied. The higher the elasticity degree of the textile, the more buckling is achievable (Table 3). The same applies to the textile thickness, where fabrics with a thickness of 5–20 deniers, perform much better than thicker fabrics (40 deniers and above). In contradiction to the formal vocabulary described by Aldinger et al. [22], the vocabulary described here is much more complex and polymorphous, as it varies in relation to the materiality of textile and fibres. In contradiction to their findings, we have observed that boundaries around the pattern geometries play an important role in the shape of the finalised panel.

This becomes evident in experiment 4, where variant v4.2 with no boundaries, did not manage to deliver the desired shape, while variants v4.3 and v4.4 which include a boundary came very close to the digital 3D model.

Furthermore, all three 3D printers (the Ultimaker 3 and the low budget printers JG and Zaxe) performed well and were able to 3D print on the textiles safely. Printing directly on the textile proved to be much more effective than laminating the pattern with glue, as the glued composites delivered less buckling in the *z*-direction (e.g. v8.1, v8.2 and v8.3, in Table 3).

Finally, one could highlight the variety of forms that are made possible by combining these two materials into a composite object; the semi-elastic Thermoplastic Polyurethane 95 and the elastic fabric. Forms that apply to rules and material properties, as well as to pattern geometry and design (Fig. 14). The success or failure of the final composite relies on the right proportion of design intentions and respect to the natural material memory and behaviour. This would allow us to enhance Frei Otto's call for lighter, more energy-saving, more mobile and more adaptable, in short, more natural buildings, or building components, such as roofs, ceilings, shading devices, tents, roofs and temporary shelters.

The limitations of this research project are linked to the size of all produced objects which is no bigger than 25 cm, which is the maximum printable size by the available 3D printers as well as a minimum rod thickness of 0.6 mm, linked to the minimum printable thickness by the printers. Our future plans include experimentation with larger-scale 3D printed objects, in order to verify our findings on a larger, architectural scale as well as examining the possibility of applying robotic technology for achieving more complex and reliable components.



Fig. 14 Variety of forms and design made possible by Methods 1 and 2

Acknowledgements We would like to express our acknowledgements to Darshan Chiba, Ffion Morris and Elliott Ward for executing experiment 1, Pattanan Inharwararak, Jinbi Jiang and Zili Qiu for executing experiment 2. Joseph Eyres, Viktor Lepetilo and Maxine Tai for executing experiment 3, Allena Anna Alphy, Diya Manoj Kulkarni and Poojapriyam Ravi from the Liverpool School of Architecture for executing experiment 4. Many thanks to Yorgos Berdos and Cesar Cheng for producing Fig. 1 and Mohannad Altabbal, Danial Mahabadi, Shreyans Mehta, Alejandro Ramirez, Ben Prescott, Jake Rothwell, Paul Nolan, Sami Samawi for producing the wearables on Fig. 14. Furthermore, our acknowledgements go to Furkan Sinan Üğütmen, Nezihe Gökçe Kökcan, Hilal Kaleli, Bilge Belenli, İrem Uysal, Yağmur Kaynar, Gözde Damla Turhan, Ece Küreli who acted as assistants for experiments 5, 6, 7 and 8 as well as Hugh Clarke, Filiz Keyder Özkan, Onur Dinmez, Çağlar Şendikici, Ayşe Bozkurt Karal from the Izmir University of Economics who executed experiments 5, 6, 7 and 8.

References

1. Einstein A (1921) Geometry and experience. Retrieved from https://www.relativitycalculator.com/pdfs/einstein_geometry_and_experience_1921.pdf
2. Massey J (2006) Buckminster Fuller's cybernetic pastoral: the United States Pavilion at Expo 67. *J Archit* 11(4):463–483. <https://doi.org/10.1080/13602360601037883>

3. Otto F, Rasch B, Schanz S (1995) *Finding form: towards an architecture of the minimal*. Edition Axel Menges, Berlin
4. Brown A, Rice P (2001) *The engineer's contribution to contemporary architecture*: Peter Rice. Thomas Telford, London
5. Wu JJ, Huang LM, Zhao Q, Xie T. (2018) 4D printing: history and recent progress. *Chin J Polym Sci* 36:563–575. <https://doi.org/10.1007/s10118-0182089-8>
6. Agkathidis A, Berdos Y, Brown A (2019) Active membranes: 3D printing of elastic fibre patterns on pre-stretched textiles. *Int J Archit Comput* 17(1):74–87. <https://doi.org/10.1177/1478077118800890>
7. Berdos Y, Agkathidis A, Brown A (2020) Architectural hybrid material composites: computationally enabled techniques to control form generation. *Archit Sci Rev* 63(2):154–164. <https://doi.org/10.1080/00038628.2019.1666357>
8. Joshi S, Rawat K, Karunakaran C, Rajamohan V, Mathew AT, Kozioł K, Thakur VK, Balan ASS (2020) 4D printing of materials for the future: Opportunities and challenges. *Appl Mater Today* 18. <https://doi.org/10.1016/j.apmt.2019.100490>
9. Cheng T, Wood D, Wang X, Yuan PF, Menges A (2020) Programming material intelligence: an additive fabrication strategy for self-shaping biohybrid components. In: Vouloutsis V, Mura A, Tauber F, Speck T, Prescott TJ, Verschure PFMJ (eds) *Biomimetic and biohybrid systems: living machines*, vol 12413 (Lecture notes in computer science). Springer, Cham. https://doi.org/10.1007/978-3-030-64313-3_5
10. Cheng T, Wood D, Kiesewetter L, Oezdemir E, Antorveza K, Menges A (2021) Programming material compliance and actuation: hybrid additive fabrication of biocomposite structures for large-scale self-shaping. *Bioinspi Biomim*. <http://iopscience.iop.org/article/10.1088/1748-3190/ac10af>
11. Meyer P, Döpke C, Ehrmann A (2019) Improving adhesion of three-dimensional printed objects on textile fabrics by polymer coating. *J Eng Fibers Fabr*, January. <https://doi.org/10.1177/1558925019895257>
12. Redondo FL, Giaroli MC, Villar MA de AGO, Ciolino AE, Ninag MD (2020) Direct 3D printing of poly (lactic acid) on cotton fibers: characterization of materials and study of adhesion properties of the resulting composites. *Macromol Symp* 394:1900190. <https://doi.org/10.1002/masy.201900190>
13. Sitotaw DB, Ahrendt D, Kyosev Y, Kabish AK (2020) Additive manufacturing and textiles. *Appl Sci* 10(15):5033. <https://doi.org/10.3390/app10155033>
14. Ehrmann G, Ehrmann A (2020) Shape-memory properties of 3D printed PLA structures. In: *Proceedings of the first international conference on “green” polymer materials*, 5–25 November 2020, MDPI: Basel, Switzerland. <https://doi.org/10.3390/CGPM2020-07198>
15. Giglio A, Paoletti I, Conti GM (2021) Three-dimensional textiles in architecture and fashion design: a brief overview of the opportunities and limits in current practice. *Appl Compos Mater*. <https://doi.org/10.1007/s10443-021-09932-9>
16. Erioli A, Naldoni L (2017) Informed flexible matter workshop. <http://www.co-de-it.com/WorkPress/informed-flexible-matter.html>
17. Guberan C, Clopath C (2016) Active shoes. <https://selfassemblylab.mit.edu/active-shoes>. MIT Self-Assembly Lab
18. Jourdan D, Skouras M, Vouga E, Bousseau A, (2021). Printing-on-fabric meta-material for self-shaping architectural models. In: *Advances in architectural geometry*, Paris, France, pp 1–19 (hal-02925036)
19. Koch HC, Schmelzeisen D, Gries T (2021) 4D textiles made by additive manufacturing on pre-stressed textiles: an overview. *Actuators* 10:31. <https://doi.org/10.3390/act10020031>
20. Goudswaard M, Abraham A, Goveia da Rocha B, Andersen K, Liang R (2020) FabriClick: interweaving pushbuttons into fabrics using 3D printing and digital embroidery. In: *Proceedings of the 2020 ACM designing interactive systems conference*. Association for Computing Machinery, New York, NY, USA, 379–393. <https://doi.org/10.1145/3357236.3395569>

21. Kycia A (2019) Hybrid textile structures as means of material-informed design strategy. In: Ballestrem M, Borrego I, Fioretti D, Pasel R, Weidinger J (eds) CA2RE Berlin proceedings: conference for artistic and architectural (doctoral) research, Berlin. Universitätsverlag der TU Berlin, pp 34–35
22. Aldinger A, Margariti A, Koerner S, Suzuki A, Knippers, J (2018) Tailoring self-formation: fabrication and simulation of membrane-actuated stiffness gradient composites. In: Creativity in structural design. Boston. https://www.researchgate.net/publication/326552014_Tailoring_SelfFormation_fabrication_and_simulation_of_membraneactuated_stiffness_gradient_composites